NASA Technical Memorandum 102386
AIAA-90-0741

Nonintrusive Inertial Vibration Isolation Technology for Microgravity Space Experiments

Carlos M. Grodsinsky and Gerald V. Brown
Lewis Research Center
Cleveland, Ohio

Prepared for the
28th Aerospace Sciences Meeting
sponsored by the American Institute of Aeronautics and Astronautics
Reno, Nevada, January 8-11, 1990

NASA

NONINTRUSIVE INERTIAL VIBRATION ISOLATION TECHNOLOGY FOR MICROGRAVITY SPACE EXPERIMENTS

Carlos M. Grodsinsky and Gerald V. Brown

National Aeronautics and Space Administration
Lewis Research Center
Cleveland, Ohio 44135

E-5127

Abstract

The dynamic acceleration environment observed on Space Shuttle flights to date and predicted for the Space Station has complicated the analysis of prior microgravity experiments and prompted concern for the viability of proposed space experiments requiring long-term, microgravity environments. Isolation systems capable of providing significant improvements to this environment exist, but at present have not been demonstrated in flight configurations. This paper presents a summary of the theoretical evaluation for two one degree-of-freedom (DOF) active magnetic isolators and their predicted response to both direct and base excitations. These isolators can be used independently or in consort to isolate acceleration-sensitive microgravity space experiments. Dependent on the isolation capability required for specific experimenter needs.

Nomenclature

c	electro-magnet damping coefficient
F	direct disturbance
F_s	isolator force
g_o	acceleration of the Earth
i_b	magnetic-circuit current bias
I_{avv}	electro-magnet current (α velocity)
K	passive stiffness coefficient
k_a	magnetic-circuit current amplifier stiffness
k_{eq}	magnetic-circuit isolator stiffness
k_g	magnetic-circuit proportional gain
k_i	magnetic-circuit current stiffness
k_p	magnetic-circuit sensor amplifier gain
k_r	magnetic-circuit derivative gain
k_θ	magnetic-circuit position stiffness
m	mass
N	number of ampere turns
u	position of base
x	position of payload
ξ_1	passive damping coefficient
τ_1	time constant of sensing circuit
τ_2	time constant of differentiator
ψ	magnetic field strength
ω	excitation frequency
ω_n	system resonance frequency
ω_{na}	active system resonance frequency

Introduction

Interest in vibration isolation for microgravity experiments has increased within the microgravity science community as the flight program has progressed and the small, but significant levels of residual acceleration on the Space Shuttle (STS) have become more widely recognized and documented.[1,2] These background accelerations result from several sources characteristic of the orbiting carrier and the orbital environment. Very low frequency (10^{-3} Hz to dc) accelerations due to drag, tidal effects, and gravity gradients contribute sub-micro-g/g_o levels. STS thruster activity can contribute 10^{-4} to 10^{-2} g/g_o accelerations with significant duration, but can be predicted and controlled. The most significant and troublesome contribution to most experiments is the moderate frequency (10^{-3} to 100 Hz) dynamic spectrum of accelerations having magnitudes in the range 10^{-5} to 10^{-2} g/g_o. This dynamic background is due primarily to random excitations from manned activity on the orbiter as well as small thruster firings for orbit keeping maneuvers. However, orbiter structure and flight systems also contribute observable intermittent and resonant accelerations to the background as the orbiter interacts with its dynamic mechanical and thermal environment.

The evolution of the Space Station design has led to many discussions of the potential limitations on long term, low gravity experimentation in this environment. It is now obvious that most of the true microgravity experiments will require isolation from this random milli-g environment if valid and reproducible results are to be expected. Because a large part of the transient disturbances have a frequency range from milli-Hz to 1 Hz, it is extremely difficult to design passive isolation systems with a resonance frequency at most $1/\sqrt{2}$ times the lowest excitation frequency of interest, mainly the sub-Hz range.

The serious limitation of passive isolators is the absence of materials which have useful ranges of both low-modulus (providing low frequency) and appropriate damping (to avoid large amplitude oscillation). Two-stage passive isolators can decrease the frequency range, however limited damping leads to potentially unstable systems in the random excitation environment. It is apparent that a passive isolation system would not suffice because of the requirement for an extremely low stiffness for the isolation of small disturbance frequencies for typical values of mass associated with microgravity space experiments. However, when

there are direct disturbances to a payload, a small value of stiffness is not desirable. Therefore, there is a trade off, and an optimal design would need to compensate for both direct disturbances, if present, and low frequency base disturbances. Thus, active systems offer significant advantages over passive systems in the orbital acceleration environment, due to both the extremely small stiffnesses needed to isolate against such low frequency base disturbances and the ability to adapt to direct disturbances for the optimal isolation of a payload, since the responses to these two excitations require conflicting solutions.

Such active systems require sensing of motion or position, and a feedback and/or a feedforward control loop to counteract mechanical excitation and minimize motion of an isolated body. Such systems introduce the complexity of a high-gain control system, but offer significant advantages in versatility and performance.[3]

This paper summarizes the theoretical evaluation of both a fully magnetically suspended one DOF system and a passive static support system with inertial electromagnetic damping. The fully magnetically suspended system is evaluated using an attractive electromagnet, while the electromagnetically damped system is evaluated using a Lorentz magnet. Magnetic systems of the attractive type have been used to suspend rotating shafts for a number of years and the required negative feedback loops to control such systems have been discussed in numerous papers, giving the equivalent stiffness and damping coefficients for specific controllers. However, these studies have not treated the isolation of the suspended body from both direct and base excitations and the response of such generic suspension systems to these types of disturbances has not been documented. Therefore the dynamic response to base and direct disturbances of both systems has been evaluated. In addition to the dynamic response of such systems, this paper deals with specific isolation needs for microgravity experiments and describes the design of a specific control technique being developed at NASA Lewis Research Center. The systems analyzed can be represented by an isolator between a base support and the isolated payload as shown in Fig. 1. The isolator is simply an actuator which is driven in proportion to certain feedback signals depending on the desired response of the payload. For the attractive magnetic actuator, it is assumed that both the stiffness and damping coefficients are derived from a relative position sensor. For the electromagnetic damping isolator, a Lorentz actuator is analyzed where the damping coefficient is derived from an inertial sensor and the stiffness is simply that of a passive spring.

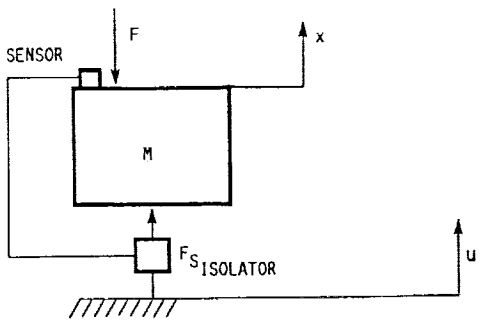

FIGURE 1. - PHYSICAL REPRESENTATION OF ACTIVE ISOLATION SYSTEMS.

The primary thrust in this activity involves the use of digital active control on dependent multidegrees of freedom. As part of the project a six DOF system will be tested under a full six DOF free fall condition, using the NASA Lewis Learjet, to acquire the coupled response between all six DOF in a low gravity environment.

Statement of the Problem

To categorize the disturbances which are present in the Space Shuttle and will be present in the Space Station, the accelerations are grouped into three frequency ranges:[4]

(1) Quasi-static external disturbances
(2) Low frequency vibration sources
(3) Medium-high frequency vibrations

Quasi-static external disturbances include aerodynamic drag, gravity gradient effects and photon pressure accelerations. The second category include excitations due to large flexible space structures, crew motion, spacecraft attitude control and robotic arms. The third catagory include disturbances due to on-board equipment such as pumps and motors having a frequency range of about 10 Hz and above (see Appendix[1,3,5]).

Overview

The active isolators described in this paper are effective at frequencies above a hundreth or a tenth of a Hz. This constraint arises not from technology limitations, but from practical limitations on the stroke needed to isolate against the very low frequencies. Volume constraints in the Shuttle and in the future Space Station manned environment laboratory modules limit the stroke of any support system. Aerodynamic drag, for example, acts on a solar pointing Station with a frequency equal to that of the orbital frequency, about 90 min per orbit. Although drag is a function of the atmospheric conditions during a specific mission, an average magnitude of 10^{-7} g/g_o will be used for the sake of argument. Thus, the distance the station would travel under such an acceleration would be $x = (a/\omega^2)2 = 1.5$ m (4.7 ft), not including initial conditions. Thus, an "isolated" payload would be forced to follow such a large spacecraft displacement and be active in a much smaller region. This active region would depend on the volume constraints of a payload in the Shuttle or Space Station microgravity module.

The following two cases, assuming use of an attractive electromagnet and a Lorentz force actuator, respectively, can be analyzed as spring-mass damper systems. It is assumed that the spring and damper characteristics are actively controlled and translated into actuator response by a control law depending on the response characteristics desired. Using an attractive electromagnet actuator, one can produce forces in only one direction. Therefore, to achieve a push-pull configuration one needs to use two electromagnets acting on an armature. For these actuators, the force produced by one magnet is proportional to the square of the current and inversely proportional to the square of the gap. Figure 2 shows the magnetic-circuit actuator's

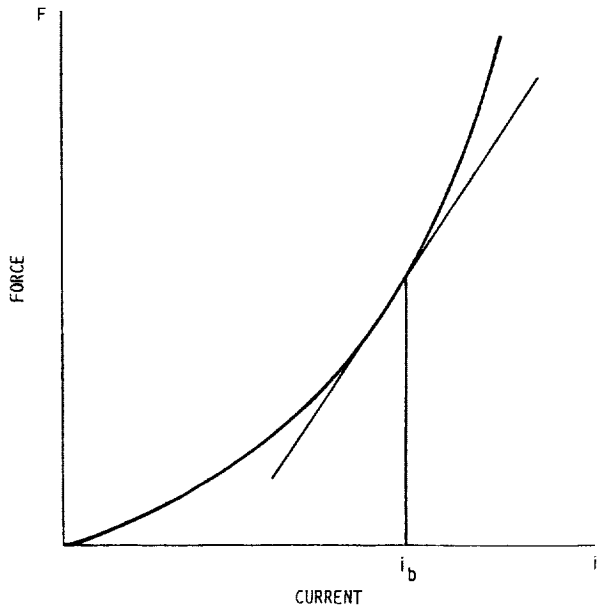

FIGURE 2. - MAGNETIC-CIRCUIT ACTUATORS SQUARED DEPENDENCE ON CURRENT.

squared dependence on current. Due to these nonlinear characteristics, a bias current linearization technique is utilized. Thus, the current bias i_b is used to produce a nearly linear control law such that for small disturbances about this current the control force produced can be assumed linear. In order to control this system, one must close a control loop around position and velocity feedback signals with a bias current so as to work in the more linear regime of the force versus current plot of a magnetic-circuit as shown in Fig. 2. Other nonlinearities arise between magnetic flux and input coil current due to hysteresis and saturation.

In contrast, the Lorentz actuator can produce forces bidirectionally. The force produced by a Lorentz actuator is a vector quantity equal to the cross product of current and field, ψ. Therefore, depending on the direction of current flow in the coil one can produce a force in either a positive or negative direction. Due to this actuator's linear dependence on control current, linearization is not needed and this actuator is open loop stable. The Lorentz actuator thus has advantages over the magnetic-circuit but requires more power to produce a certain force than does the magnetic-circuit configuration. However, the forces needed to control a payload in the weightless environment of space are small and this inefficiency is not as limiting as on the Earth.

The basic concept behind these active isolation techniques is the sensing of position, velocity and/or acceleration and driving an actuator 180° out of phase with this signal in order to cancel a disturbance to the payload. If there is knowledge about certain disturbances, a feedforward loop can anticipate an excitation and react without an error signal. Thus, the optimal dynamic response for microgravity experiments, to known and sensed orbiter environments, would result from the inertial isolation of a body by a feedforward/feedback type controller. Such a controller does not circumvent the need for relative information of the payload in order to follow the large motion disturbances without exceeding boundary conditions, (i.e., volume constraints). These active isolation techniques can be implemented using either analog or digital control schemes to close the feedback or feedforward control loops.

The control laws in one DOF for the magnetic-circuit isolator and for a Lorentz electromagnetically damped system are described by their transmissibilities and effectiveness in isolating against both base and direct disturbances. To summarize, these transmissibilities and effectiveness functions are given with a brief description of their formulation. First, the responses or transmissibilities of both systems will be generated for harmonic base excitations, using the active isolation system's differential equations of motion. These equations of motion were written using Newton's first and second laws, where the base displacement, u, is actually a time function, so $u = u(t)$ with the same implied for a directly applied force, such that in actuality $F = F(t)$. Therefore, for a spring mass damper system, the equations of motion for base excitation become:

Magnetic-Circuit Isolator

$$m\frac{d^2x}{dt^2} + k_{eq}(x - u) + c_{eq}\left(\frac{dx}{dt} - \frac{du}{dt}\right) = 0 \qquad (1)$$

Electromagnetic Damping Isolator

$$m\frac{d^2x}{dt^2} + c\frac{dx}{dt} + Kx = Ku \qquad (2)$$

These systems look very similar to passive viscoelastic systems with the exception that, for all practical purposes, both the stiffness and damping of either isolator can be set as desired. By joining these control methods appropriately one can produce an active system with variable stiffness and damping referenced to inertial space. Therefore, these systems can be easily configured as adaptive systems where, by using sensed information from the disturbance environment, the control law could be changed to optimize the isolation of the payload. In the magnetic-circuit actuator, the stiffness and damping are not strictly independent, but the dependence is minimal if certain control parameters are met. (For example, a certain amount of damping is needed in order to overcome instabilities.) To achieve a purely damped response independent of stiffness, be it active or passive stiffness, one would need to use a Lorentz actuator.

In defining the dynamic base motion equations for both systems, the stiffness and damping terms can be found by using the appropriate control law needed for a stable negative feedback system. The stiffness and damping solutions for both cases are summarized in a paper which is in preparation.[6] However, the stiffness and damping coefficients for the magnetic-circuit isolator case are derived in a similar manner to those which arise for a magnetic bearing configuration, and such derivations can be found in many papers on the subject of magnetic bearings; for example, Ref. 7.

In summary, the stiffness coefficient for the magnetic-circuit becomes:

$$k_{eq} = k_\theta + \frac{k_i k_a k_p\left[k_g\left(1 - \tau_2\tau_1\omega^2\right) + \left(k_g + k_r\right)\left(\tau_2 + \tau_1\right)\tau_2\omega^2\right]}{\left(1 - \tau_2\tau_1\omega^2\right)^2 + \left(\tau_2 + \tau_1\right)^2\omega^2} \quad (3)$$

For the electromagnetic isolator, because the mass is being statically supported by a passive spring, the stiffness is simply K. Summarizing the damping coefficients for both isolators, the magnetic-circuit damping coefficient becomes

$$c_{eq} = \frac{k_i k_a k_p\left[\left(1 - \tau_2\tau_1\omega^2\right)\left(k_g + k_r\right)\tau_2 - k_g\left(\tau_2 + \tau_1\right)\right]}{\left(1 - \tau_2\tau_1\omega^2\right)^2 + \left(\tau_2 + \tau_1\right)^2\omega^2} \quad (4)$$

and the electromagnetic damping

$$c = -\psi N I_{avv} \qquad \text{where:} \qquad I_{avv} = \frac{E_{avv}}{R} \quad (5)$$

(note: calculations assume negligible inductance)

As one can see, the magnetic-circuit actuator system is more complex than the Lorentz actuator due to the nonlinear characteristics of the magnet. Also, since the stiffness is a function of the excitation frequency, the natural frequency of this system is not constant. However, for small excitation frequencies, which is the range of interest, the natural frequency of the system can be assumed constant.

In order to solve the equations by defining the base excited system transfer function, the dynamic equations will be transformed into the frequency domain using the Laplace transformation:

$$F(s) = \int_{-\infty}^{\infty} F(t)e^{-st}\,dt \quad (6)$$

Then, transforming the transfer functions into vibration notation, the two equations become:

Magnetic-Circuit Transfer Function

$$\frac{X}{U}(s) = \frac{2\xi\omega_n s + \omega_n^2}{s^2 + 2\xi\omega_n s + \omega_n^2} \quad (7)$$

Electromagnetic Damping Transfer Function

$$\frac{X}{U}(s) = \frac{\omega_n^2}{s^2 + 2\xi\omega_n s^2 + \omega_n^2} \quad (8)$$

The frequency response for both functions is obtained from the relation:

$$\frac{X}{U}(j\omega) = \lim_{t\to\infty}\left[\frac{X}{U}(s)\right] \text{ for } s = j\omega \quad (9)$$

where: $j = \sqrt{-1}$

Thus, the transfer functions in terms of frequency response are vectors in the complex plane and the magnitudes of vibration measured on the isolated payload resulting from a sinusoidal excitation usin(ωt) is the vector length of X/U(jω). This value, a scalar, is called the transmissibility function of the system. The transmissibility is generally written as $T = \left|\frac{X}{U}(j\omega)\right|$. Therefore, the transmissibility functions become:

Magnetic-circuit Transmissibility Function

$$T = \left|\frac{X}{U}(j\omega)\right| = \sqrt{\frac{1 + \left(2\xi\frac{\omega}{\omega_n}\right)^2}{\left[1 - \left(\frac{\omega}{\omega_n}\right)^2\right]^2 + \left(2\xi\frac{\omega}{\omega_n}\right)^2}} \quad (10)$$

Electromagnetic Damping Transmissibility Function

$$T_{av} = \left|\frac{X}{U_{av}}(j\omega)\right| = \frac{1}{\sqrt{\left[1 - \left(\frac{\omega}{\omega_n}\right)^2\right]^2 + \left(2\xi\frac{\omega}{\omega_n}\right)^2}} \quad (11)$$

By plotting these transmissibilities, one can see the effect of changing the stiffness or damping of either system. The transmissibility curve for the first case, shown in Fig. 3, illustrates the effect of increasing the damping coefficient of the

$$\xi = \frac{K_i K_g K_p[(K_g + K_r) - K_g 1.022]10^{-3}}{(1 - \tau_2\omega^2)^2 + (\tau_2 + \tau_1)^2\omega^2}$$

$$\omega_n^2 = K_\theta + \frac{K_i K_g K_p\left[K_g(1 - \tau_2\tau_1\omega^2) + (K_g + K_r)(\tau_2 + \tau_1)\tau_2\omega^2\right]}{(1 - \tau_2\omega^2)^2 + (\tau_2 + \tau_1)^2\omega^2}$$

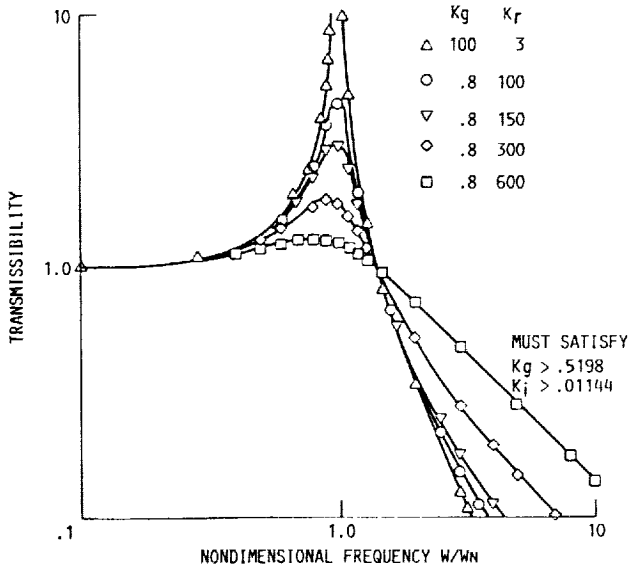

FIGURE 3. - RELATIVE FEEDBACK TRANSMISSIBILITY CURVES.

magnetic-circuit isolator system. The curves show that with enough velocity feedback gain, K_r, the system can become overly damped, which gives rise to a well damped resonance but less isolation at excitation frequencies above $\sqrt{2}$ times ω_n than would be achieved with a less damped system. The effect of increasing or decreasing the position gain, K_g, is to shift the natural frequency of the system to the right or left because of the change in equivalent stiffness.

The effect of increasing the damping coefficient of the Lorentz electromagnetic damping system, is illustrated in Fig. 4. The curves show

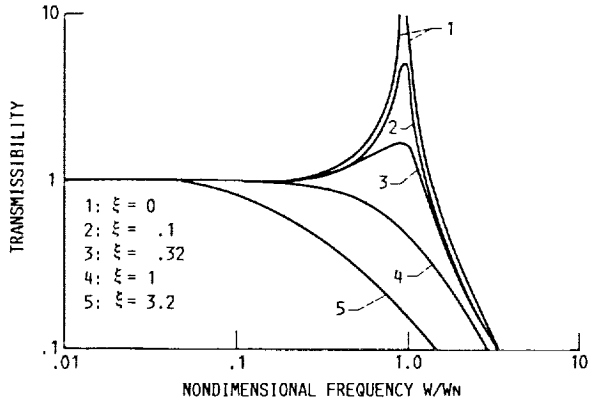

FIGURE 4. - INERTIAL DAMPING TRANSMISSIBILITY CURVES.

the response of the system to increased velocity feedback, i.e., damping determined from the integration of an inertial sensor signal. The great advantage of active damping derived from an inertial reference is that it removes the resonant response, broadening and smoothing the transition between the low frequency and high frequency regions, while reducing both the transmission and the response, particularly in the low frequency range of interest. The effects of such a system for large values of velocity feedback gain can be understood by noting that it is equivalent to having a passive damper attached between the isolated mass and a virtual inertial reference. As the damping is increased, the isolated mass becomes more and more tightly coupled to the (motionless) ideal inertial reference. Unlike the passive damper placed between the experiment and the vibrating base, the stronger the damping, the better the isolation. This type of response is not seen in the pure suspension case because the velocity term was determined from the derivative of a relative position sensor giving rise to the response shown in Fig. 3.

In order to relate these curves to the microgravity environment, one can use a g/g_o versus frequency plot, which was generated from typical Microgravity Science Laboratory acceleration data[1,2] measured on a shuttle flight, and superimpose the transmissibility curves on this data to predict the isolation performance achievable for such disturbances. By superimposing these curves, one can get a rough idea of the capability of such a system in isolating against such low frequency disturbances. These curves are presented in Fig. 5.[1,3] Figure 5 shows selected peak accelerations (open data points) typical of those observed on STS missions[1,3] and an upperbound (line with positive slope) that is intended to reflect the

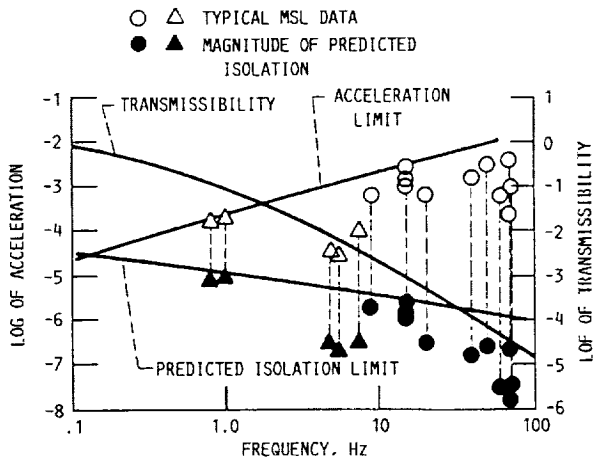

FIGURE 5. - INERTIAL DAMPING TRANSMISSIBILITY AND PREDICTED ACCELERATION RESPONSE.

"worst case" limit for such an environment. The filled data points show the effect of filtering this "mechanical noise" through the Lorentz isolator and the resultant "worst case" line.

As explained previously, these curves all demonstrate system response to base excited harmonic motions. However, disturbances may also be generated directly on the payload itself. The sensitivity of the isolated payload to a disturbing force will be characterized by a term called the isolated payload mobility. The mobility of the payload is the vector magnitude of $X(s)/F(s)$.

This parameter measures the amplitude of the payload deflection per unit of force amplitude. The equations of motion for both systems, for direct disturbance only are:

Magnetic-Circuit Equation of Motion

$$M\frac{d^2x}{dt^2} = F(t) - K_{eq}x - C_{eq}\frac{dx}{dt} \qquad (12)$$

Electromagnetic Damping Equation of Motion

$$M\frac{d^2x}{dt^2} = F(t) - Kx - c\frac{dx}{dt} \qquad (13)$$

These equations can be placed in the Laplace operation format and from the definition of the vector magnitude $X(s)/F(s)$, one can write the mobility equation for both cases as follows:

Magnetic-circuit Mobility Equation

$$\frac{X(s)}{F(s)} = \frac{1}{Ms^2 + C_{eq}s + K_{eq}} \qquad (14)$$

Electromagnetic Damping Mobility Equation

$$\frac{X(s)}{F(s)} = \frac{1}{Ms^2 + cs + K} \qquad (15)$$

In order to evaluate the effectiveness of these active systems, the ratio of $X(s)/F(s)$ active to $X(s)/F(s)$ for a typical passive system will be used. This ratio will be called the mobility effectiveness $X_f(s)$. Therefore, if $X_f(s)$ is

unity, the active system behaves the same as the passive one. If $X_f(s)$ is zero, no motion of the payload results from a finite applied force. If $X_f(s)$ is greater than unity, then the active system amplifies the effect of the applied force, increasing the payload motion. The equations for the effectiveness function for both cases, in terms of frequency response, where the vector length of $X_f(s)$ is $\left|\bar{X}_f(j\omega)\right|$, become:

Magnetic Circuit Effectiveness

$$\left|X_f\left(\frac{j\omega}{\omega_n}\right)\right| = \frac{\omega_n}{\omega_{na}} \sqrt{\frac{\left[1 - \left(\frac{\omega}{\omega_n}\right)^2\right]^2 + \left(2\xi_1 \frac{\omega}{\omega_n}\right)^2}{\left[1 - \left(\frac{\omega}{\omega_n}\right)^2_a\right]^2 + \left(2\xi \frac{\omega}{\omega_n}\right)^2_a}} \qquad (16)$$

where for small excitation frequencies $\omega_{na} \approx \omega_n$

ξ_1 = damping coefficient of passive spring

(A value of 0.05 was used for ξ_1.)

$$\text{Active } \omega_n = \sqrt{\frac{K_{eq}}{M}};\ \frac{C_{eq}}{M} = 2\xi\omega_n$$

Electromagnitic Damping Effectiveness

$$\left|\bar{X}_f\left(\frac{j\omega}{\omega_n}\right)_v\right| = \sqrt{\frac{\left[1 - \left(\frac{\omega}{\omega_n}\right)^2\right]^2 + \left(2\xi_1 \frac{\omega}{\omega_n}\right)^2}{\left[1 - \left(\frac{\omega}{\omega_n}\right)^2\right]^2 + \left(2\xi \frac{\omega}{\omega_n}\right)^2}} \qquad (17)$$

where $\frac{c}{M} = 2\xi\omega_n$; $\omega_n = \sqrt{\frac{K}{M}}$; $\xi = \frac{1}{2} G_v \sqrt{\frac{1}{KM}}$

ξ_1 = damping coefficient of passive spring

(A value of 0.05 was used for ξ_1.)

These effectiveness functions are plotted in Figs. 6 and 7. Figures 6 and 7 present the effectiveness of the active feedback, force actuated vibration isolation systems as compared to a passive system with a critical damping coefficient of 0.05, which is typical for passive systems of the type utilized with low frequency system resonances.

As shown by the transmissibility curves in Figs. 3 and 4, there are many advantages in developing isolation systems with the specific characteristics of both active relative and inertial closed loop isolation systems. To date there have been systems developed which exploit inertial damping methods however, their limitations arise from the cut off frequencies obtainable because of the passive stiffness utilized for static support of the payload. Such a passive stiffness can be physically described in terms of a classical spring where the stiffness must be large enough to support the constant loading a payload is to experience and thus, this required stiffness dictates the dynamic stiffness of the system, once a transient disturbance is introduced. However, by actively supporting the payload with an integral term of the

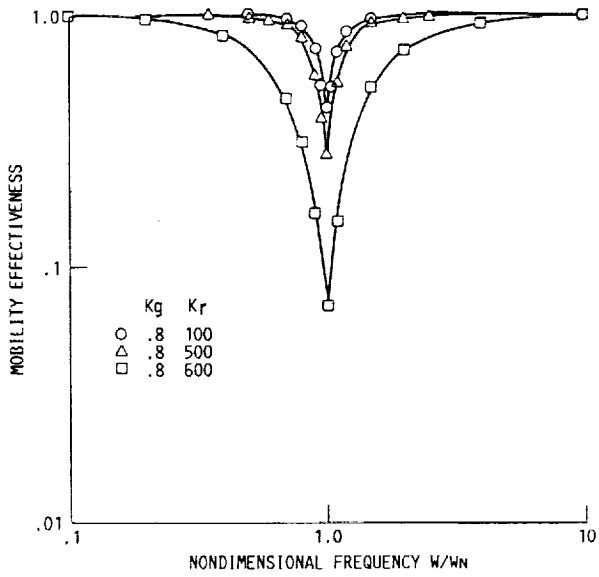

FIGURE 6. - RELATIVE FEEDBACK MOBILITY EFFECTIVENESS CURVES.

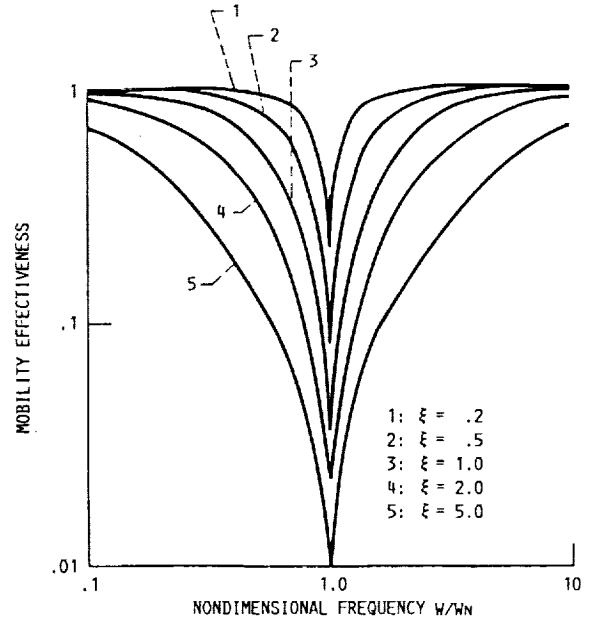

FIGURE 7. - INERTIAL DAMPING MOBILITY EFFECTIVENESS CURVES.

relative position, and setting the relative position gain term appropriately, one can tailor the effective dynamic stiffness of a system to whatever value is desired, dependent on the user's requirements. In effect, one can design an active support system with classical isolation characteristics with the versatility of changing the dynamic stiffness and damping parameters independantly to produce a desired response. This gives the ability to set the cut off frequency of such a system to much lower values, if the appropriate strokes are obtainable in the working volume of the payload. However, for such a relative sensor defined control system, increasing the damping gain term gives rise to better response at resonance, but impedes isolation at frequencies above $\sqrt{2}$ times ω_n. This response arises from taking the relative velocity of the system which manifests itself in the $2\xi\omega/\omega_n$ term in the numerator of Eq. (10), shown in Fig. 3.

In developing an appropriate control logic for optimal payload isolation, an accelerometer referenced to the moving frame is joined with a relative sensor needed for support, in a feedforward capacity. By adding the appropriate integral of the inertial sensor to the appropriate relative information, one can obtain the inertial isolation response of Figs. 4 and 7 nonintrusively. Isolating in such a manner, one can configure a system independent of the actual payload and by digitally controlling such a system, the appropriate parameters can be programmed for specific requirements.

Summarizing this nonintrusive inertial isolation control approach, one can see that the equation of motion for a typical suspension configuration, Eq. (1), must be changed to have the following form:

$$m\frac{d^2x}{dt^2} + k_{eq}(x - u) + c_{eq}\left(\frac{dx}{dt}\right) = 0 \qquad (18)$$

To design this system with the equivalent equation of motion shown above, one must configure the closed loop control system around both a relative and inertial sensor, where these sensors give the relative position of the payload with respect to the dynamic support and the support's acceleration, respectively. By using this information as the feedback/feedforward control signals one arrives at the following equation of motion for such a system:

$$m\frac{d^2x}{dt^2} + k_{eq}(x - u) + c_{eq}\left(\frac{dx}{dt} - \frac{du}{dt}\right) + c_{eq}\left(\frac{du}{dt}\right) = 0 \qquad (19)$$

The control block diagram for this control system is shown in Fig. 9. In utilizing this concept, a six DOF system was designed for laboratory development and is currently 80 percent complete. Active control of three DOF has been demonstrated, including the implementation of the inertial active vibration isolation control. The remaining DOF will be added in the subsequent months as the remaining hardware is fabricated and integrated into the laboratory test bed.

Concluding Remarks

In conclusion, it is apparent that the active magnetic systems described here have advantages over passive isolators due to their ability to isolate against the low frequencies present on the orbital carriers, as well as their ability to implement an adaptive control to isolate against both the direct and base excitations which will be present in all pressurized modules. Therefore, it is apparent that the optimal isolation of microgravity science payloads will require an adaptive digitally controlled system to optimize isolation coefficients so as to most effectively prevent disturbances from perturbing the payload. To lower the corner frequencies of such an active system, one would need to use actuators with larger and larger strokes. However, because of the volume constraints present in space flight vehicles, an isolated payload will have to follow these very low

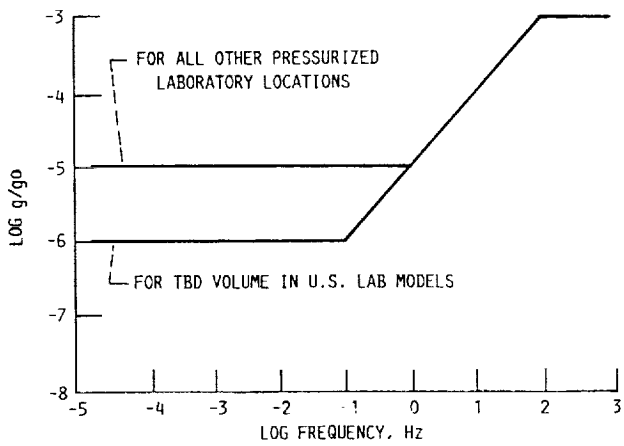

FIGURE 8. - SPACE STATION FREEDOMS MICROGRAVITY REQUIREMENT.

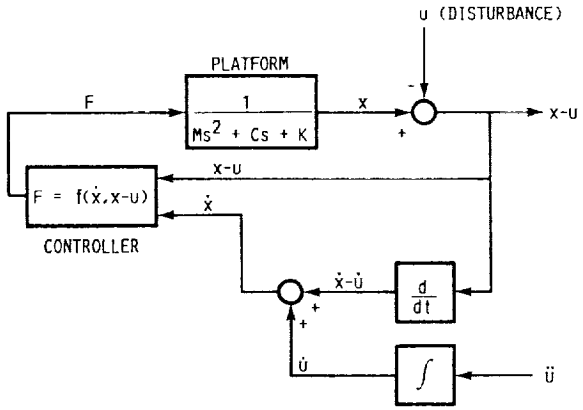

FIGURE 9. - ONE-DOF INTERTIAL CONTROL SYSTEM.

steady-state accelerations, resulting from aerodynamic drag, gravity gradient effects, etc. To achieve the microgravity requirements imposed on the Space Station facility (Fig. 8) for any significant length of time, microgravity vibration isolation will have to become a systems engineered solution as well as an experiment-specific concern. Thus, the requirements for acceleration-sensitive microgravity space experiments will dictate multistage isolation concepts which will combine both passive and active systems where the control of the center of gravity of Space Station will be closed around such microgravity steady-state accelerations.

Appendix

The range of accelerations which have been observed on several STS missions or estimated for the accessible orbit are summarized below:[1,3,5]

Quasi-steady or "dc" acceleration disturbances

g/go	Frequency, Hz	Source
10^{-7}	0 to 10^{-3}	Aerodynamic drag
10^{-8}	0 to 10^{-3}	Light pressure
10^{-7}	0 to 10^{-3}	Gravity gradient

Periodic acceleration disturbances

g/go	Frequency, Hz	Source
2×10^{-2}	9	Thruster fire (orbital)
2×10^{-3}	5 to 20	Crew motion
2×10^{-4}	17	Ku band antenna

Nonperiodic acceleration disturbances

g/go	Frequency, Hz	Source
10^{-4}	1	Thruster fire (attitude)
10^{-4}	1	Crew push off

References

1. Hamacher, H., "Simulation of Weightlessness," Materials Sciences in Space," B. Feuerbacher, H. Hamacher, and R.J. Naumann, eds., Springer-Verlag, New York, 1986, pp. 31-51.

2. Workshop Proceedings: "Measurement and Characterization of the Acceleration Environment on Board the Space Station," Aug. 11-14, 1986, Guntersville, Al.

3. Ruzicka, J.E., "Active Vibration and Shock Isolation," SAE Paper 680747, 1969.

4. Jones, D.I., Owens, A.R., Owen R. G., and Roberts, G., "Microgravity Isolation Mount," ESA CR(P)-2480, European Space Agency, Paris, France, 1987.

5. Hamacher, H., Feuerbacher, B., and Jilg, R., "Analysis of Microgravity Measurements in Spacelab," Proceedings of the Fifteenth International Symposium on Space Technology and Science, vol. 2, H. Matsuo, ed., Tokyo, Japan, 1986, pp. 2087-2097.

6. Grodsinsky, C., "Development and Approach to Low Frequency Microgravity Isolation Systems," NASA TM, in preparation 1989.

7. Humphris, R.R., Kelm, R.D., Lewis, D.W., and Allaire, P.E., "Effect of Control Algorithms on Magnetic Journal Bearing Properties," Journal of Engineering for Gas Turbines and Power, vol. 108, no. 4, Oct. 1986, pp. 624-632.

NASA
National Aeronautics and Space Administration

Report Documentation Page

1. Report No.	2. Government Accession No.	3. Recipient's Catalog No.
NASA TM-102386 AIAA-90-0741		

4. Title and Subtitle	5. Report Date
Nonintrusive Inertial Vibration Isolation Technology for Microgravity Space Experiments	6. Performing Organization Code

7. Author(s)	8. Performing Organization Report No.
Carlos M. Grodsinsky and Gerald V. Brown	E-5127
	10. Work Unit No. 694-03-03

9. Performing Organization Name and Address	11. Contract or Grant No.
National Aeronautics and Space Administration Lewis Research Center Cleveland, Ohio 44135-3191	13. Type of Report and Period Covered Technical Memorandum

12. Sponsoring Agency Name and Address	14. Sponsoring Agency Code
National Aeronautics and Space Administration Washington, D.C. 20546-0001	

15. Supplementary Notes

Prepared for the 28th Aerospace Sciences Meeting sponsored by the American Institute of Aeronautics and Astronautics, Reno Nevada, January 8-11, 1990.

16. Abstract

The dynamic acceleration environment observed on Space Shuttle flights to date and predicted for the Space Station has complicated the analysis of prior microgravity experiments and prompted concern for the viability of proposed space experiments requiring long-term, microgravity environments. Isolation systems capable of providing significant improvements to this environment exist, but at present have not been demonstrated in flight configurations. This paper presents a summary of the theoretical evaluation for two one degree-of-freedom (DOF) active magnetic isolators and their predicted response to both direct and base excitations. These isolators can be used independently or in consort to isolate acceleration-sensitive microgravity space experiments. Dependent on the isolation capability required for specific experimenter needs.

17. Key Words (Suggested by Author(s))	18. Distribution Statement
Vibration isolators; Vibration damping; Microgravity experiments; Active, Adaptive control; Electromagnetics	Unclassified - Unlimited Subject Category 31

19. Security Classif. (of this report)	20. Security Classif. (of this page)	21. No of pages	22. Price*
Unclassified	Unclassified		

*For sale by the National Technical Information Service, Springfield, Virginia 22161